Journal of chemical & engineering data

Article

pubs.acs.org/jced

Density Measurements of Propellant EHF-TU at (3 to 7) MPa Supercritical Pressures

Jie Wen, Nan Zhang, Yanchen Fu,* Guoqiang Xu, Haoran Huang, and Xiaojun Yan

National Key Laboratory of Science and Technology on Aero-Engine Aero-Thermodynamics, School of Energy and Power Engineering, Beihang University, Beijing, 100191, China

ABSTRACT: Endothermic Hydrocarbon Fuel-Tianjin University (EHF-TU) is one advanced propellant and fractionated from RP-3 extensively used in China. The density of propellant EHF-TU at supercritical pressures is measured using the flow conservation method. The measurement covers temperatures from (303 to 765) K and pressures of (3 to 7) MPa using three tubes with different sizes, and the density varies from (759 to 134) kg·m^{-3}. The *n*-decane is used for calibration, and the relative uncertainty of density measurement is 1.1%. A series of measures were adopted to improve the measurement accuracy including flexible sizes of test tubes, the lumped parameter method, and the advanced data process. The results indicate that density decreases with the decline of temperature and pressure. Dramatic variation of density occurs in the pseudocritical region at 3 MPa pressure. Density data is fitted using polynomials, and the average absolute deviation (AAD) between the experimental data and the fitted data is 0.7%. Additionally, the volumetric thermal expansion coefficient of EHF-TU is calculated using the polynomials.

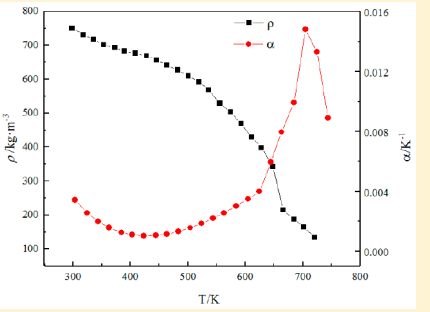

1. INTRODUCTION

In recent decades, the flight speed of aircrafts has experienced rapid development from subsonic to supersonic to hypersonic. With the development of engines, the turbine heat load will rapidly increase due to the increase in turbine inlet temperature. The turbine inlet temperature was 1100 K in the 1950s and is expected to reach 2300 K by 2020.[1] To meet the needs of the turbine inlet temperature and pressure ratio's improvement, the cooled cooling air (CCA) technology is proposed. The CCA technology is to improve the cooling air's quality with the smallest technical risk and weight, by using the own fuel as a cold source through heat exchangers installed in aero engines.[2] There are currently many mainstream propellants like JP-8 and Chinese RP-3. New and advanced propellants are still being studied. When the multicomponent hydrocarbon fuel absorbs heat, the temperature rises and eventually is beyond the critical value. In this process, the fluid exhibits a series of special characteristics, especially the dramatic variations in thermal properties. As thermal properties are researched on the basis of flow and heat transfer, these variations could lead to peculiar phenomena at supercritical pressures. The database of fluid thermal properties mainly includes density,[3] specific heat,[4−7] dynamic viscosity,[8−10] thermal conductivity,[11−13] vapor pressure,[14−16] and critical properties.[17] Accurate measurement of thermal properties is needed to perform numerical simulations and shorten the design cycle of heat-exchangers in aero engines.

Density is an important property parameter in scientific and engineering applications. The measurement method of the density is divided into two categories: one is the direct measurement based on the relationship of quality and volume $\rho = \frac{m}{V}$, and the other one is the indirect measurement based on the relationship of density and other physical quantities.[20−22,30] The densities of pure substances[18−20] and mixtures[3,21−29] have been investigated by many researchers. Dai et al.[20,21] measured the density of the mixture of CO_2 and styrene at 313/323/333/343 K with a maximum pressure of 34.47 MPa. Yun et al.[22] measured the density of the binary mixture of ethane and its cosolvent. The experimental temperature remained constant at 308.2 K, and the pressure varied from (4.98 to 10.57) MPa. Bruno et al.[30] tested the hydrocarbon fuel JP-10 density using the SVM3000 and DSA5000 instruments and formed a technical report. The maximum positive and negative errors are 0.04 and −0.22%, respectively. Yang et al.[31] measured the hydrocarbon fuel temperature from (283 to 950) K and pressure of (3 to 4) MPa using a gamma densitometer.

An indirect measurement like the vibration method can measure the density of fluid under high pressure but cannot be used under high temperature conditions. In a word, these methods mostly are suitable for low temperature, high pressure or high temperature, low pressure conditions of density measurement. In this work, a novel method to measure the density under high pressure and temperature conditions was proposed and updated. During the experiments, the operating pressures were at supercritical status and varied from (3 to 7) MPa, and the fluid temperature was varied from (303 to 765) K.

Received: December 19, 2017
Accepted: May 14, 2018

DOI: 10.1021/acs.jced.7b01097
J. Chem. Eng. Data XXXX, XXX, XXX−XXX

2. EXPERIMENTAL SECTION

2.1. Materials. EHF-TU (Endothermic Hydrocarbon Fuel-Tianjin University) is a specific aerospace propellant developed by Tianjin University. Furthermore, EHF-TU is used as an important coolant for thermal protection scheme designing in the regenerative cooling and cooled cooling air (CCA) technologies. It mainly consists of naphthenic hydrocarbon (51.3%), alkane (48.2%), and aromatic hydrocarbon (0.5%). The boiling range of EHF-TU is listed particularly in Table 1, and the

Table 1. Boiling Range of EHF-TU

boiling range (K)	magnitude
455.7	initial boiling point
471.1	10%
477.2	20%
486.0	50%
504.9	90%
528.0	end boiling point

Table 2. Detailed Compositions of EHF-TU

no.	composition	mass fraction
1	*n*-dodecane	21.93
2	*n*-hendecane	14.49
3	*n*-tridecane	7.519
4	1-methyl-decahydronaphthalene	4.723
5	7-methyldotridecane	4.274
6	hexylcyclohexane	4.000
7	2,6-methyldodecane	3.800
8	decahydronaphthalene	3.115
9	*cis*-2-methyl-decahydronaphthalene	2.936
10	2-methylundecane	2.700
11	3-methyldecane	2.560
12	*trans*-2-methyl-decahydronaphthalene	2.249
13	1,1-methyl-2-pentyl-3-methyldodecane	2.236
14	*n*-decane	2.165
15	2-ethyl-decahydronaphthalene	1.839
16	3-methyldodecane	1.674
17	2,3-methyl-decahydronaphthalene	1.653
18	isobutylcyclohexane	1.236
19	2-methyldodecane	1.138
20	4-methyldecane	1.132
21	pentylcyclohexane	0.728
22	1-methyl-2-pentylcyclohexane	0.417
23	6-methyluntridecane	0.311
24	others	11.18

detailed compositions of EHF-TU are listed in Table 2. Density, as one of the most important thermal physical properties, directly influences the heat transfer coefficient. The detailed density data need to be known to provide the basis for the design of thermal protection.

2.2. Experimental System. Figure 1 shows the supercritical hydrocarbon fuel flow and heat transfer system at Beihang University. It consists of five sections: preparative system, preheat section, test section, reclaimed section, and data collection system. In the preparative system, the fuel is pumped up by a high pressure constant current pump (SP6015, 15 MPa, 0.01−600.00 mL·min^{-1}; LP-0110, 15 MPa, 0.01−999.99 mL·min^{-1}). The pump is followed by a filter with a net spacing of 45 μm to protect the pump from logging of impurities in the fuel and ensure the safe operation of the experimental system. The mass flow rate is measured by a Coriolis-force flow meter (model, DMF-1-1, ±0.15%), and the range is 0−0.005 and 0−0.01 kg·s^{-1}. The preheat section consists of two 20 kW adjustable DC powers (TN-KGZ01, 100 V, 200 A) and heats the fuel to a maximum of 873 K. The test section is covered by Aspen (thermal conductivity of 0.012 W·m^{-1}·K^{-1}) to reduce the heat loss. There is an absolute pressure gauge at the exit of the test section to measure the system pressure. The system pressure is controlled by a back pressure valve. The high-temperature fuel after the test section flows through a water-cooled heat exchanger and is cooled to 310 K. The cooled fuel directly discharged into a waste oil tank. The electrical signals are collected by Adam-4018 and stored on computers by Adam-4520 during the experiments.

2.3. Test Section. The test section is a straight tube made of stainless steel 1Cr18Ni9Ti with various sizes. Three different kinds of tubes were used during the whole measurement for different flow bulk temperature regions, and detailed parameters are listed in Table 3. The inner diameter is measured using the scanning electron microscope (SEM) and shown in Figure 2. The length and inner diameter variations could meet the requirement of fully developed turbulent flow and ensure the adequate flowing residence time. Thus, the measurement accuracy could be guaranteed and will be discussed later.

Figure 3 presents the detail of the test section. Sections A and D are the inlet and outlet of the fluid, respectively. There are metal nets for mixing the fluid evenly in the B and C regions. The test section is wrapped with a tropical belt to offset the heat loss so that the import and export temperatures basically remained the same (the deviation is less than 1 K). There is a heating section before the test tube for the generation of temperature pulses. The armored thermocouples' wire diameter is 1 mm to guarantee the rapid response time and keep the measurement accuracy at the high level. Flow bulk temperature variations are collected, transferred, and stored as electrical signals through the "Beihang Intelligent Sensor" with a maximum frequency of 200 Hz.

Figure 4 shows results of electrical signals before and after filter. The electrical signals are subject to significant interference with a fluctuation range of approximately 0.04 mV (1 K). After adding the low-pass filter, the signal fluctuation is reduced to 0.006 mV (0.15 K).

The thermocouple calibration curve is shown in Figure 5 in the temperature range from (273 to 773) K. The uncertainty of temperature measurement is less than ±0.5% in the range (273 to 423) K, ±0.4% in the range (423 to 573) K, and ±0.27% in the range (573 to 773) K.

3. THEORY AND UNCERTAINTY ANALYSIS

3.1. Theory. The density measurements are derived from the mass conservation. The average velocity can be calculated as follows.

$$U(T) = \frac{L}{\Delta t} \quad (1)$$

L and Δt are the length of the test section and the flowing residence time in the test section, respectively. At a certain temperature, the incompressible fluid flows through a tube and the mass conservation formula is

$$\dot{m} = \rho(T)U(T)A \quad (2)$$

DOI: 10.1021/acs.jced.7b01097
J. Chem. Eng. Data XXXX, XXX, XXX−XXX

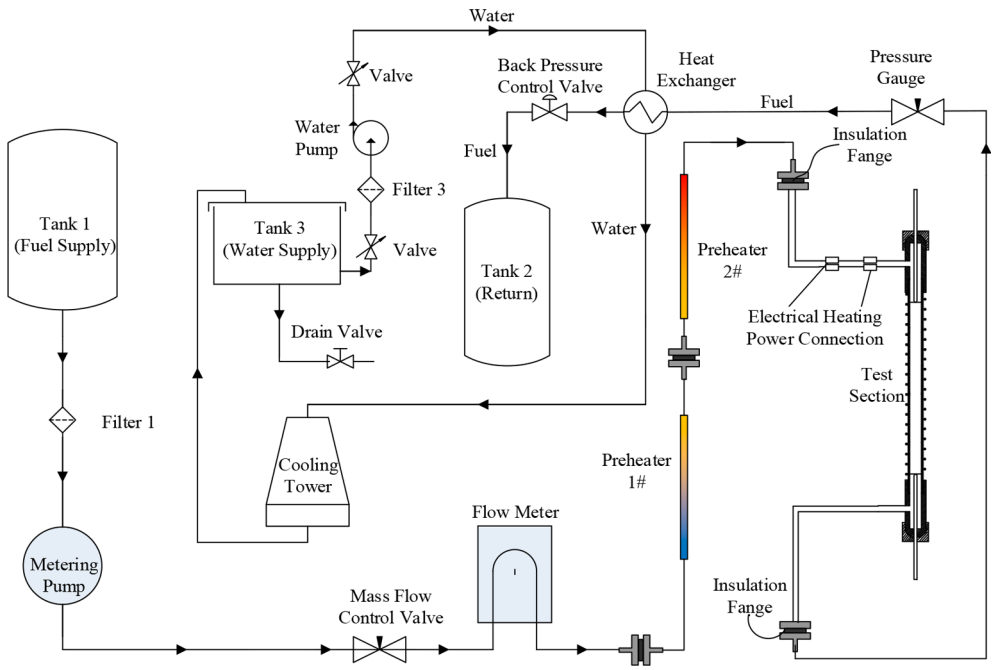

Figure 1. Schematic of supercritical hydrocarbon fuel flow and heat transfer system.

Table 3. Parameters of Three Sizes of Test Tubes and Corresponding Temperature Regions

no.	L (mm)	d (mm)	D (mm)	temperature region (K)
1	2045	2.995	4	303−363
2	1160	4.121	6	363−563
3	556	5.913	8	563−783

where $\rho(T)$ and $U(T)$ are the density and average velocity. $\dot{m}$ and A are the mass flow rate and the cross-sectional area, respectively. The density of the fluid can be calculated using the following equation.

$$\rho(T) = \frac{\dot{m}\Delta t}{LA} \tag{3}$$

For a smooth circular tube, its flow area is defined as

$$A = \frac{\pi d^2}{4} \tag{4}$$

Thus, the density measurement formula is transferred as below.

$$\rho = 4\frac{\dot{m}\Delta t}{\pi d^2 L} \tag{5}$$

3.2. Lumped Parameter Method. The Reynolds number in a tube is calculated as follows

$$\mathrm{Re} = \frac{4\dot{m}}{\eta\pi d} \tag{6}$$

where $\dot{m}$ is the mass flow rate, η is the fluid dynamic viscosity, and d is the inner diameter of the tube.

When the fluid flows through the top of thermocouples, the convective heat transfer phenomenon exists. Nu is the Nusselt number defined in the following equation[32]

$$Nu = \frac{hd}{\lambda} = C\mathrm{Re}^n\mathrm{Pr}^{1/3}$$
$$C = 0.683,\ n = 0.466 \quad \mathrm{Re} = 40-4000$$
$$C = 0.193,\ n = 0.618 \quad \mathrm{Re} = 4000-40000 \tag{7}$$

where λ is the fluid thermal conductivity and h is the heat transfer coefficient.

The Biot number is calculated as follows

$$Bi = \frac{hR_s}{\lambda_s} \tag{8}$$

where R_s and λ_s are the radius and thermal conductivity of the armored thermocouple wire, respectively. For the n-decane and

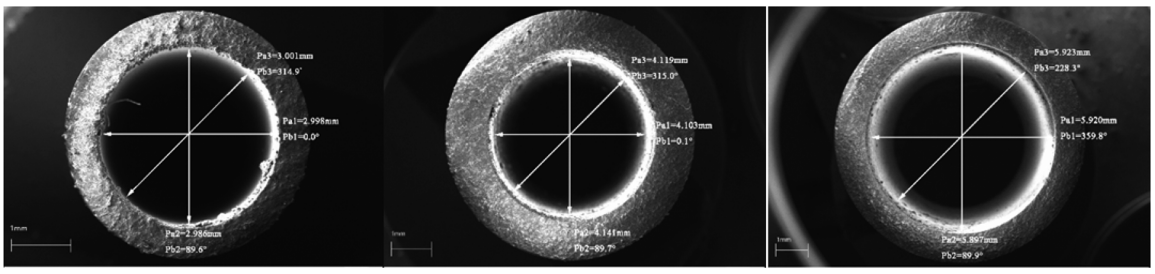

Figure 2. Inner diameter photograph by SEM (left, 2.995 mm; middle, 4.121 mm; right, 5.913 mm).

DOI: 10.1021/acs.jced.7b01097
J. Chem. Eng. Data XXXX, XXX, XXX−XXX

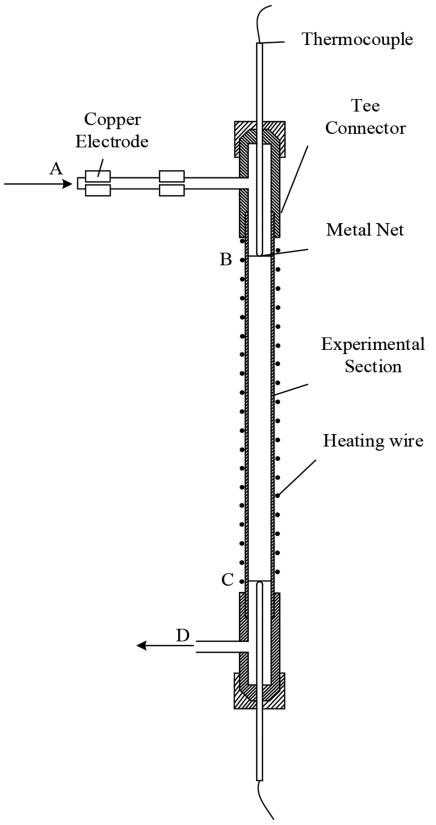

Figure 3. Schematic of test section. A, the inlet; B, the start point of test section; C, the end point of test section; D, the outlet.

EHF-TU, Bi is about 0.01−0.025 and 0.01−0.02 in the temperature range from (300 to 700) K, respectively. The condition $Bi \leq 0.1$ is satisfied for the whole experimental situations, and the lumped parameter method can be adopted in the density measurements.

The thermocouple time constant τ_c is calculated in the following equation

$$\tau_c = \frac{\rho c V}{hA} \tag{9}$$

where ρ and c are the density and isobaric specific heat capacity of fluid, respectively, and V and A are the volume and surface area of the thermocouple's top. The thermocouple theory response relation is

$$\frac{T - T_0}{T_f - T_0} = 1 - e^{-\tau/\tau_c} \tag{10}$$

where T is the fluid transient temperature. T_0 and T_f are the initial temperature and the real temperature, respectively. τ is the measurement time. For n-decane, the time constant is τ_c = (0.09 to 0.16) s in the temperature range. For EHF-TU, the time constant is τ_c = (0.11 to 0.15) s.

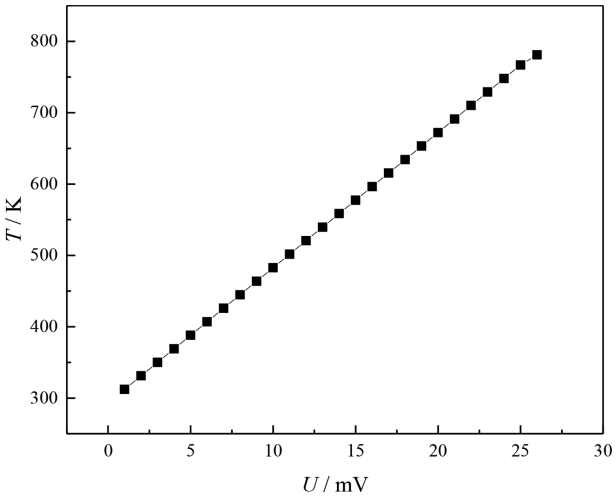

Figure 5. Variations of temperature T versus the thermocouple's voltage U. T = 18.905U + 293.585.

3.3. Uncertainty Analysis. The uncertainty analysis is finished according to the procedures given by Li et al.[33,34] The tube length, inner diameter, and mass flow rate are directly measured in the experiments. Direct measuring uncertainties are listed in Table 4.

Table 4. Uncertainty of Direct Measurements

direct measurement	measuring uncertainty
tube length L	1 mm
tube inner diameter d	0.001 mm
mass flow rate $\dot{m}$	0.15%

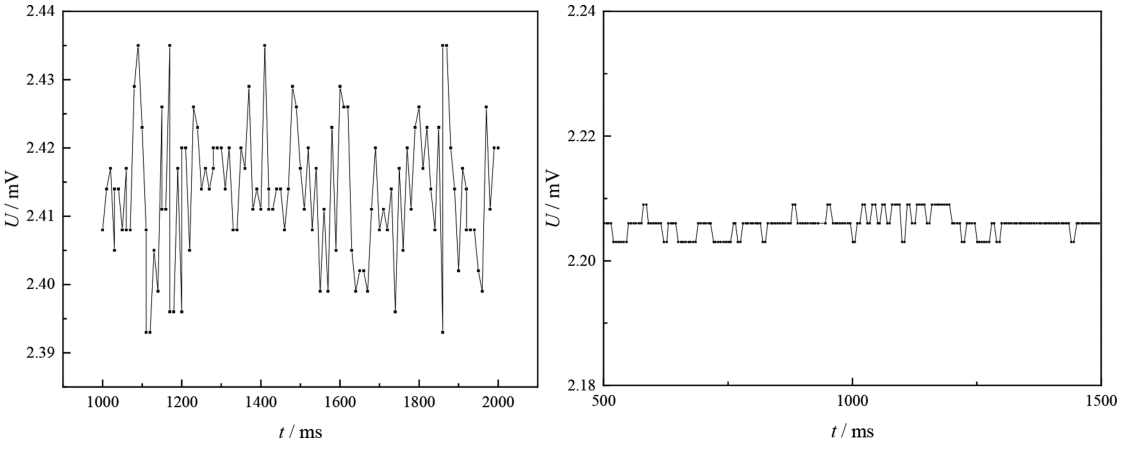

Figure 4. Contrast of electrical signal voltage U versus time t before and after the filter.

DOI: 10.1021/acs.jced.7b01097
J. Chem. Eng. Data XXXX, XXX, XXX−XXX

If the transient temperature $T - T_0$ is 0.15 K and the time constant is 0.16 s, the thermocouple response time is 2.4 ms, less than the measurement error of 5 ms caused by the acquisition card. In the experiment, the residence time under all conditions is more than 1 s in the temperature range. The measurement error of the residence time Δt is within ±0.5%.

The relative uncertainty of density measurement is calculated as follows according to eq 5.

$$\varepsilon(\rho) = \sqrt{\varepsilon(\dot{m})^2 + \varepsilon(L)^2 + 4\varepsilon(d)^2 + \varepsilon(\Delta t)^2} \quad (11)$$

Thus, the uncertainty value is calculated as 0.55%. The coverage factor is $k = 2$, and the relative expanded uncertainty of density measurement is $u_r(\rho) \approx 0.01\rho$.

3.4. Density Data Processing Method. According to the description in section 3.1, the vital important step on the density measurement is to achieve the accurate residence time. Figure 6

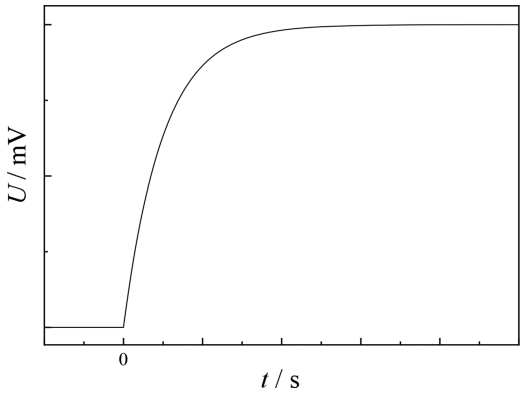

Figure 6. Variations of the thermocouple's voltage U versus time t in the ideal situation. The solid line shows the theoretical response curve.

shows the theoretical response curve in the ideal situation when thermocouples are suddenly put into the high-temperature fluid. At $t = 0$, the thermocouple voltage signal suddenly rises and its first derivative is discontinuous.

As shown in Figure 7, the slope of the response curve gradually increases due to the sudden variation of the fluid temperature and the influence of the thermocouple's heat capacity. The fluctuation of the voltage signal becomes smaller after the filter. The wavelet type is DB3, and the threshold level is 5. When the artificial starting points are selected, the error is inevitably increasing. This paper presents two rules to determine the starting point of the response: The first one is to select the thermocouple data within a certain time before the response and take the average. The second one is to select the intersection point between the mean and the far right lines of the response curve. The difference between the starting point for the response of the import and export is the residence time. This method can eliminate the error caused by manual selection.

4. RESULTS AND DISCUSSION

4.1. Calibration. The density of the *n*-decane (the purity is 98.7%) is measured at temperatures from (285 to 723) K and 3 MPa pressure. The pseudocritical temperature is 648.2 K at 3 MPa. The phase is liquid when the temperature is lower than 648.2 K, and the *n*-decane is in the supercritical state when the temperature is higher than 648.2 K. The experimental density, theoretical density, and relative deviation are listed in Table 5.

Table 5. Experimental Density ρ_{exp}, Theoretical Density ρ_{real}, and RD $= \frac{\rho_{exp} - \rho_{real}}{\rho_{real}} \times 100\%$ of *n*-Decane at Pressure $P = 3$ MPa and Temperature $T = (285$ to $723)$ K[a]

T (K)	ρ_{exp} (kg·m^{-3})	ρ_{real} (kg·m^{-3})	RD (%)
285.3[b]	736.80	738.66	−0.25
313.1[b]	716.24	717.48	−0.17
343.4[b]	706.6	694.21	1.78
354.5[b]	682.30	685.58	−0.48
373.3[b]	660.16	670.79	−1.58
423.7[b]	630.21	630.43	−0.03
475.8[b]	588.61	585.76	0.49
523.2[b]	547.44	537.31	1.89
571.8[b]	487.16	476.13	2.32
624.2[b]	365.90	366.27	−0.10
673.2[c]	143.74	141.75	1.40
700.3[c]	112.44	112.98	−0.48
723.0[c]	96.77	99.63	−2.87

[a]The relative expanded uncertainties u_r are $u_r(T) = 0.005$ and $u_r(P) = 6.5 \times 10^{-4}$, and the relative expanded uncertainty U_r is $U_r(\rho) = 0.01$ (0.95 level of confidence). [b]Liquid. [c]Supercritical state.

The theoretical density is calculated by NIST-Refprop.[35] The relative deviation (RD), average absolute deviation (AAD), and maximum absolute deviation (MAD) are calculated as follows.

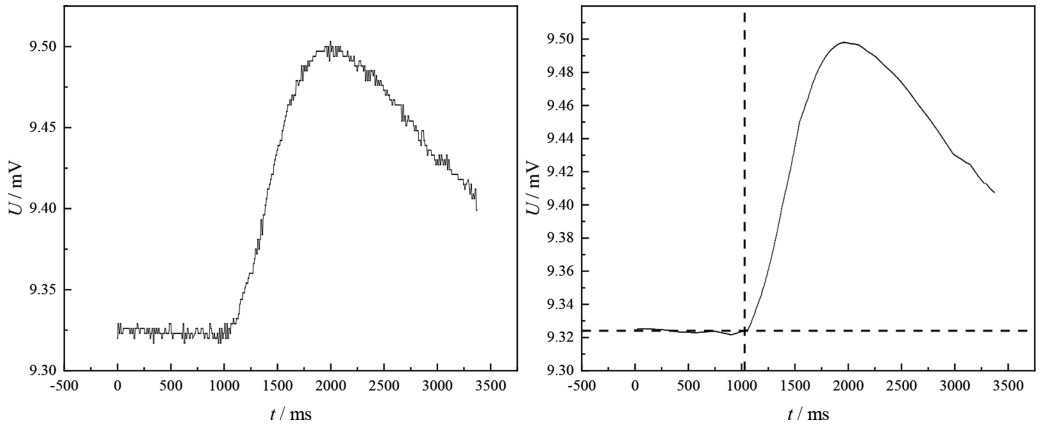

Figure 7. Variations of the thermocouple's voltage U versus time t. Left: solid line, response curve in the measurement. Right: solid line, response curve after filter; horizontal dashed line, the average voltage; vertical dashed line, the starting point of response.

DOI: 10.1021/acs.jced.7b01097
J. Chem. Eng. Data XXXX, XXX, XXX−XXX

$$\mathrm{RD} = \frac{\rho_{\mathrm{exp}} - \rho_{\mathrm{real}}}{\rho_{\mathrm{real}}} \times 100\% \quad (12)$$

$$\mathrm{AAD} = \frac{100}{n} \sum_{i=1}^{n} \left| \left(\frac{\rho_{\mathrm{exp},i} - \rho_{\mathrm{real},i}}{\rho_{\mathrm{real},i}} \right) \right| \quad (13)$$

$$\mathrm{MAD} = \max\left(\left| \frac{\rho_{\mathrm{exp},i} - \rho_{\mathrm{real},i}}{\rho_{\mathrm{real},i}} \right| \right) \quad (14)$$

As shown in Figure 8, the AAD of the *n*-decane is 0.99% and the MAD of the *n*-decane is 2.9%. In the low-temperature region

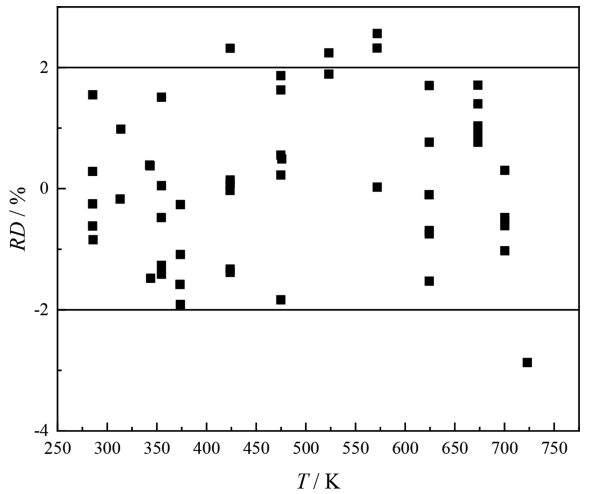

Figure 8. Deviation of experimental and theoretical density $\mathrm{RD} = \frac{\rho_{\mathrm{exp}} - \rho_{\mathrm{real}}}{\rho_{\mathrm{real}}} \times 100\%$ of *n*-decane at pressure P = 3 MPa and temperature T = (285 to 723) K.

(T < 285 K), the measured value deviates greatly from the theoretical value. When the fluid temperature is low, due to the large fluid viscosity, the Reynolds number is low, and the flow is in laminar or transition state. According to eq 2, the flow rate measured by the inlet and outlet thermocouple response times is the fluid average velocity. The flow velocity in a tube is not equal everywhere at the cross section. The center flow velocity is larger than the surrounding flow rate, especially in the laminar flow state. As the diameter of the thermocouple is much smaller than the diameter of the tube, the thermocouple is not guaranteed to be exactly in the center of the tube. Therefore, it is necessary to ensure the Reynolds number is large enough to obtain accurate measurement results. At the same time, the Reynolds number cannot infinitely increase because short residence time will enlarge the measurement error. Due to the pump's restriction, the Reynolds number cannot be enough in the low-temperature region (T < 300 K). Thus, three sizes of tubes were chosen to ensure enough Reynolds numbers influenced by inner diameter and residence time influenced by the length of the tube at temperatures of (300 to 765) K.

After the calibration, the following principles are summarized and applied to ensure the minimum measurement error: (1) Use a high-precision DC power, and add the power filter to reduce the interference. (2) The Reynolds number is in the range 5000–20000, and the residence time is (1.2 to 2.4) s. In order to achieve the required Reynolds number, three kinds of tubes with different lengths and inner diameters are designed. (3) The temperature pulse generated by the inlet fluid temperature is about 10 K. Too small temperature pulse is difficult to be measured by the thermocouple, and too large temperature pulse will change the flow state. All of these situations will increase the measurement errors. (4) Each temperature condition is measured five times, and the results are averaged to reduce the accidental error.

4.2. Density Measurement of the EHF-TU. The density of EHF-TU has been measured at temperatures of (303 to 765) K and pressures of (3 to 7) MPa. The detailed data has been listed in Table 6, and Figure 9 shows the density variation of EHF-TU with temperature. The EHF-TU is in the liquid state when the temperature is lower than the pseudocritical temperature and in the supercritical state when the temperature exceeds the pseudocritical temperature. As the temperature rises and the pressure reduces, the density of EHF-TU decreases. The critical pressure of EHF-TU is about 1.913 MPa. The density reduces drastically at about a temperature of 700 K and a pressure of 3 MPa in the pseudocritical region, and the thermal properties change drastically. When the system pressure is greater than 4 MPa, the trend of the density of EHF-TU with temperature is relatively stable and there is no significant change. The AAD between the experiment value and the fitted value is 0.75, 0.69, 0.94, 0.69, and 0.38% at various pressures. Although the relative expanded uncertainty of density measurement is small, the measurement error may increase considering the following factor: (1) The bubble caused by the cracking reaction in the high-temperature region. (2) The dramatic variation of density in the pseudocritical region. Below the pseudocritical temperature, MAD = 1.8% occurred at 3 MPa pressure. Moreover, MAD is equal to 3.5% near the pseudocritical region and MAD = 1.9% in the supercritical region. The measurement error will increase when the EHF-TU begins to crack and generate a lot of bubbles. These bubbles will influence the flow state in the tube and hinder the accurate measurement.

4.3. Volumetric Thermal Expansion Coefficient of EHF-TU. The volumetric thermal expansion coefficient is given by

$$\alpha_V = -\frac{1}{\rho}\left(\frac{\partial \rho}{\partial T}\right)_P \quad (15)$$

The subscript P means the substance expands at constant pressure. α_V can be calculated using the fitting formula at the different system pressures.

Figure 10 shows the volumetric thermal expansion coefficient of EHF-TU at supercritical pressures. When the temperature is lower than the pseudocritical temperature, the value of α_V gradually decreases and then increases as the temperature rises. When the temperature reaches the pseudocritical temperature, the α_V obviously increases due to the sharp variation of density. The results show that the value of α_V reduces with the increase of the pressure due to the decline of density sensitivity to temperature at high pressures. When the pressure is 3 MPa, there is an evident peak of the α_V, and the temperature peak (T = 704.4 K) is the pseudocritical temperature. However, there is no evident peak of α_V at P = (4 to 7) MPa. The reason is that thermal properties have no significant change when the pressure is relatively high.

5. CONCLUSION

The measurement method of density is improved to measure the density of propellant on the basis of the flow conservation at supercritical pressures. The propellant EHF-TU in liquid and

DOI: 10.1021/acs.jced.7b01097
J. Chem. Eng. Data XXXX, XXX, XXX−XXX

Table 6. Experimental Density ρ of EHF-TU at Test Pressure P = (3 to 7) MPa and Temperature T = (303 to 765) K[a]

3 MPa		4 MPa		5 MPa		6 MPa	
T (K)	ρ (kg/m^3)	T (K)	ρ (kg/m^3)	T (K)	ρ (kg/m^3)	T (K)	ρ (kg/m^3)
303.4[b]	750.650	303.4[b]	750.147	303.5[b]	750.273	303.3[b]	754.364
324.9[b]	731.064	324.5	733.028	324.4	736.181	323.4	741.045
343.8[b]	717.497	343.5	719.600	343.5	724.027	343.6	727.210
363.2[b]	701.385	363.4	705.511	363.6	707.866	363.8	712.388
384.6[b]	692.987	385.0	694.192	384.6	694.570	384.7	701.188
403.1[b]	682.690	403.2	682.816	403.0	684.952	403.3	688.974
423.4[b]	676.645	423.3	674.862	423.1	675.685	422.9	679.663
444.5[b]	669.512	444.4	664.986	444.5	666.426	444.3	673.010
463.7[b]	656.502	463.7	656.180	464.1	658.608	464.1	665.603
483.2[b]	641.513	483.4	642.285	483.5	647.429	484.1	655.939
504.0[b]	627.539	504.7	625.643	504.0	630.876	504.5	640.044
524.0[b]	609.968	523.8	613.504	523.6	618.272	523.2	625.095
544.1[b]	591.830	543.5	597.866	544.0	605.312	543.3	612.963
562.9[b]	568.781	563.6	576.225	563.4	584.427	563.6	594.642
584.1[b]	528.883	584.7	536.321	584.7	550.096	585.0	570.894
604.7[b]	503.576	603.9	508.860	604.3	520.369	604.8	544.328
624.4[b]	469.478	623.9	486.550	624.1	492.964	624.4	520.168
644.5[b]	429.586	644.8	449.603	644.8	468.931	644.9	489.303
663.2[b]	398.699	664.7	419.750	663.6	439.111	663.8	465.019
684.7[b]	343.067	684.2	387.290	683.9	415.076	683.8	442.613
704.4[b]	214.624	703.4	343.023	704.0	391.358	703.7	419.413
724.8[c]	187.845	728.3	297.938	728.2	347.751	726.3	388.250
743.7[c]	164.562	742.9	257.854	743.8	317.991	743.4	355.290
764.4[c]	134.224	765.1	187.922	765.5	243.363	765.5	294.023
7 MPa		7 MPa		7 MPa		7 MPa	
T (K)	ρ (kg/m^3)	T (K)	ρ (kg/m^3)	T (K)	ρ (kg/m^3)	T (K)	ρ (kg/m^3)
303.4[b]	758.884	423.0	687.824	543.0	617.305	663.6	470.469
324.5	744.096	444.1	679.114	563.7	599.826	684.0	450.729
343.3	730.254	464.7	668.196	584.7	577.688	703.3	430.036
363.7	717.881	483.9	658.364	603.9	551.489	725.5	401.462
384.3	707.281	504.0	644.482	624.4	524.354	744.3	381.389
403.2	696.766	523.3	630.615	645.0	496.675		

[a]The relative expanded uncertainties u_r are $u_r(T)$ = 0.005 and $u_r(P)$ = 6.5 ×10^{-4}, and the relative expanded uncertainty U_r is $U_r(\rho)$ = 0.01 (0.95 level of confidence). [b]Liquid. [c]Supercritical state.

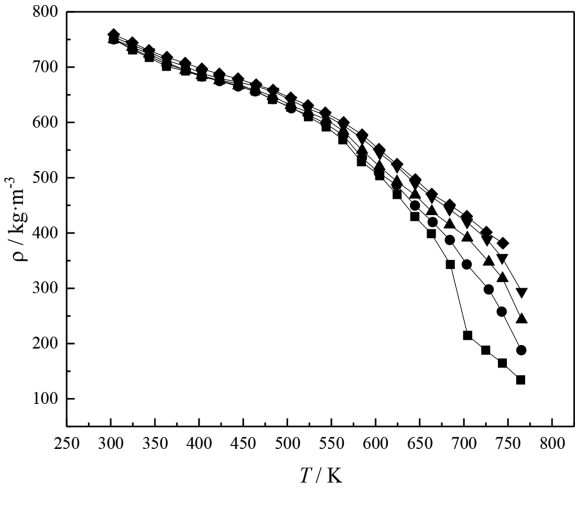

Figure 9. Experimental density ρ of EHF-TU at test pressure P = (3 to 7) MPa and T = (303 to 765) K. ■, P = 3 MPa; ●, P = 4 MPa; ▲, P = 5 MPa; ▼, P = 6 MPa; ◆, P = 7 MPa.

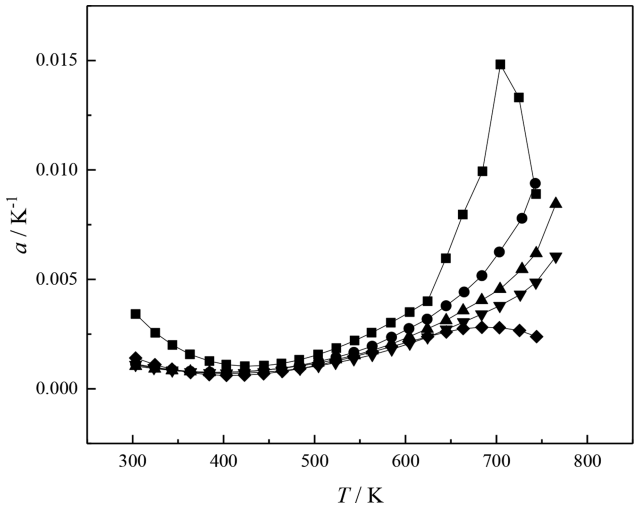

Figure 10. Volumetric thermal expansion coefficient α_V of EHF-TU at test pressure P = (3 to 7) MPa and T = (303 to 765) K. ■, P = 3 MPa; ●, P = 4 MPa; ▲, P = 5 MPa; ▼, P = 6 MPa; ◆, P = 7 MPa.

supercritical state is measured in the temperature range from (303 to 765) K and in the the pressure range from (3 to 7) MPa.

The relative uncertainty of density measurement is 1.1%. The *n*-decane is used for calibration, and the AAD is 0.99%. Many

DOI: 10.1021/acs.jced.7b01097
J. Chem. Eng. Data XXXX, XXX, XXX−XXX

measures have been adopted to decrease the measurement error, and the filter is used to pick up the starting point precisely. The values of EHF-TU are fitted using polynomials, and the AAD between the measurement value and the fitted value is 0.7%. Also, the volumetric thermal expansion coefficient α_V of EHF-TU is calculated and α_V increases with the temperature rising and decreases with the enlargement of the pressure.

AUTHOR INFORMATION

Corresponding Author

*E-mail: yanchenfu@buaa.edu.cn. Fax: +86 010-82314545.

ORCID

Yanchen Fu: 0000-0002-8145-7015

Notes

The authors declare no competing financial interest.

ACKNOWLEDGMENTS

The authors would like to thank Prof. Guozhu Liu at Tianjin University, P. R. China, for his technical support.

REFERENCES

(1) Edwards, T. USAF supercritical hydrocarbon fuels interests. 31st Aerospace Sciences Meeting, 1993, 807.

(2) Bruening, G. B.; Chang, W. S. Cooled Cooling Air Systems for Turbine Thermal Management[R]. ASME Paper, No. 99-GT-14.

(3) Deng, H. W.; Zhang, C. B.; Xu, G. Q.; Tao, G.; Zhang, B.; Liu, G. Z. Density measurements of endothermic hydrocarbon fuel at sub-and supercritical conditions. *J. Chem. Eng. Data* **2011**, *56*, 2980−2986.

(4) Tanaka, K.; Takahashi, G.; Higashi, Y. Measurements of the Isobaric Specific Heat Capacities for trans-1,3,3,3-Tetrafluoropropene (HFO-1234ze(E)) in the Liquid Phase. *J. Chem. Eng. Data* **2010**, *55*, 2267−2270.

(5) Tanaka, K.; Higashi, Y. Measurements of the Isobaric Specific Heat Capacity and Density for Dimethyl Ether in the Liquid State. *J. Chem. Eng. Data* **2010**, *55*, 2658−2661.

(6) Tanaka, K.; Higashi, Y.; Akasaka, R. Measurements of the Isobaric Specific Heat Capacity and Density for HFO-1234yf in the Liquid State. *J. Chem. Eng. Data* **2010**, *55*, 901−903.

(7) Deng, H. W.; Zhu, K.; Xu, G. Q.; Tao, Z.; Zhang, C. B.; Liu, G. Z. Isobaric specific heat capacity measurement for kerosene RP-3 in the near-critical and supercritical regions. *J. Chem. Eng. Data* **2012**, *57*, 263−268.

(8) Deng, H. W.; Zhang, C. B.; Xu, G. Q.; Zhang, B.; Tao, Z.; Zhu, K. Viscosity measurements of endothermic hydrocarbon fuel from (298 to 788) K under supercritical pressure conditions. *J. Chem. Eng. Data* **2012**, *57*, 358−365.

(9) Chen, J. T.; Chu, H. P. Densities and viscosities for binary mixtures of ethyl lactate with methacrylic acid, benzyl methacrylate, and 2-hydroxyethyl methacrylate at (298.15, 308.15, and 318.15) K. *J. Chem. Eng. Data* **2007**, *52*, 650−654.

(10) Chen, J. T.; I-Min Shiah, A.; Chu, H. P. Excess molar volumes and viscosities for binary mixtures of propylene glycol monomethyl ether with methacrylic acid, benzyl methacrylate, and 2-hydroxyethyl methacrylate at (298.15, 308.15, and 318.15) K. *J. Chem. Eng. Data* **2006**, *51*, 2156−2160.

(11) Xu, G. Q.; Jia, Z. X.; Wen, J.; Deng, H. W.; Fu, Y. C. Thermal-conductivity measurements of aviation kerosene RP-3 from (285 to 513) K at sub-and supercritical pressures. *Int. J. Thermophys.* **2015**, *36*, 620−632.

(12) Wang, Y.; Wu, J.; Liu, Z. Thermal Conductivity of Gaseous Dimethyl Ether from (263 to 383) K. *J. Chem. Eng. Data* **2006**, *51*, 164−168.

(13) Wang, Y.; Wu, J.; Xue, Z.; Liu, Z. Thermal Conductivity of HFC-245fa from (243 to 413) K. *J. Chem. Eng. Data* **2006**, *51*, 1424−1428.

(14) Wang, J. F.; Li, C. X.; Wang, Z. H.; Li, Z. H.; Jiang, Y. B. Vapor pressure measurement for water, methanol, ethanol, and their binary mixtures in the presence of an ionic liquid 1-ethyl-3-methylimidazolium dimethylphosphate. *Fluid Phase Equilib.* **2007**, *255*, 186−192.

(15) Jiang, X. C.; Wang, J. F.; Li, C. X.; Wang, L. M.; Wang, Z. H. Vapour pressure measurement for binary and ternary systems containing water methanol ethanol and an ionic liquid 1-ethyl-3-ethylimidazolium diethylphosphate. *J. Chem. Thermodyn.* **2007**, *39*, 841−846.

(16) Zhao, J.; Jiang, X. C.; Li, C. X.; Wang, Z. H. Vapor pressure measurement for binary and ternary systems containing a phosphoric ionic liquid. *Fluid Phase Equilib.* **2006**, *247*, 190−198.

(17) Sun, Q.; Mi, Z.; Zhang, X. Determination of critical properties (tc, Pc) of endothermic hydrocarbon fuels RP-3 and simulated JP-7. *J. Fuel Chem. Technol. (Beijing, China)* **2006**, *34*, 466−470.

(18) Lei, Y.; Chen, Z.; An, X.; Huang, M. J.; Shen, W. G. Measurements of Density and Heat Capacity for Binary Mixtures {x Benzonitrile + (1 − x) (Octane or Nonane)†. *J. Chem. Eng. Data* **2010**, *55*, 4154−4161.

(19) Fedele, L.; Pernechele, F.; Bobbo, S.; Scattolini, M. Compressed Liquid Density Measurements for 1,1,1,2,3,3,3-Heptafluoropropane (R227ea). *J. Chem. Eng. Data* **2007**, *52*, 1955−1959.

(20) Dai, H. J.; Heath, K. D.; Cochran, H. D.; Simonson, H. D. Density Measurements of 2-Propanol Solutions in Supercritical CO_2. *J. Chem. Eng. Data* **2001**, *46*, 873−874.

(21) Dai, H. J.; Simonson, J. M.; Cochran, H. D. Density Measurements of Styrene Solutions in Supercritical CO_2. *J. Chem. Eng. Data* **2001**, *46*, 1571−1573.

(22) Yun, S. L. J.; Dillow, A. K.; Eckert, C. A. Density Measurements of Binary Supercritical Fluid Ethane/Cosolvent Mixtures. *J. Chem. Eng. Data* **1996**, *41*, 791−793.

(23) Baylaucq, A.; Boned, C.; Dauge, P.; Lagourette, B. Measurements of the viscosity and density of three hydrocarbons and the three associated binary mixtures versus pressure and temperature. *Int. J. Thermophys.* **1997**, *18*, 3−23.

(24) Watson, G.; Zéberg-Mikkelsen, C. K.; Baylaucq, A.; Boned, C. High-pressure density measurements for the binary system ethanol+ heptane. *J. Chem. Eng. Data* **2006**, *51*, 112−118.

(25) Fandiño, O.; Comuñas, M. J. P.; Lugo, L.; Fernández, J. Density measurements under pressure for mixtures of pentaerythritol ester lubricants. Analysis of a density− viscosity relationship. *J. Chem. Eng. Data* **2007**, *52*, 1429−1436.

(26) Wang, Y.; Lian, H. L.; Luo, T. L.; Liu, G. J. Densities and Viscosities of (1, 6-Hexanediamine+ Ethanol) and (1, 6-Hexanediamine + Ethanol+ Water) Mixtures at T = (303.15 to 328.15) K. *J. Chem. Eng. Data* **2009**, *54*, 1158−1162.

(27) Outcalt, S.; Laesecke, A.; Freund, M. B. Density and speed of sound measurements of Jet A and S-8 aviation turbine fuels. *Energy Fuels* **2009**, *23*, 1626−1633.

(28) Mohsen-Nia, M.; Rasa, H. Measurements and calculations of hydrocarbon mixtures liquid density by simple cubic equations of state. *Phys. Chem. Liq.* **2009**, *47*, 140−147.

(29) Stringari, P.; Scalabrin, G.; Richon, D. Liquid Density Measurements for the Propylene + 2-Propanol + Water System. *J. Chem. Eng. Data* **2009**, *54*, 2285−2290.

(30) Bruno, T. J.; Huber, M. L.; Laesecke, A.; Lemmon, E. W.; Perkins, R. A. Thermochemical and thermophysical properties of JP-10. *Technical Report NISTIR* **2006**, *6640*, 325.

(31) Yang, Z.; Bi, Q.; Guo, Y.; Liu, Z. H.; Yan, J. G.; Zhang, Q. Design of a gamma densitometer for hydrocarbon fuel at high temperature and supercritical pressure. *J. Chem. Eng. Data* **2014**, *59*, 3335−3343.

(32) Cengel, Y. A. *Heat transfer, a practical approach*; WCB McGraw-Hill: Boston, MA, 1988; p 228

(33) Li, G. Q.; Wu, Z.; Li, W.; Wang, Z. K.; Wang, X.; Li, H. X.; Yao, S. C. Experimental investigation of condensation in micro-fin tubes of different geometries. *Exp. Therm. Fluid Sci.* **2012**, *37*, 19−28.

(34) Wu, Z.; Wu, Y.; Sundén, B.; Li, W. Convective vaporization in micro-fin tubes of different geometries. *Exp. Therm. Fluid Sci.* **2013**, *44*, 398−408.

(35) Ely, J. F.; Huber, M. L. Nist Standard Reference Database 4-Nist Thermophysical Properties of Hydrocarbon Mixtures. National Inst. of Standards: Gaithersburg, MD, 1990.

DOI: 10.1021/acs.jced.7b01097
J. Chem. Eng. Data XXXX, XXX, XXX−XXX